Heliyon 11 (2025) e42660

Contents lists available at ScienceDirect

Heliyon

journal homepage: www.cell.com/heliyon

Research article

Assessing the vulnerability of groundwater to pollution under different land management scenarios using the modified DRASTIC model in Bahir Dar City, Ethiopia

Wasie Asmamaw Ashagrie [a], Temesgen Gashaw Tarkegn [a,b,c,*], Ram Lakhan Ray [b], Gebrekidan Worku Tefera [b], Sintayehu Fetene Demessie [d,i], Lewoye Tsegaye [a], Anwar Assefa Adem [a,b], Abeyou W. Worqlul [e], Pieter R. van Oel [c], Enyew Adgo [a], Amare Haileslassie [f], Yihun T. Dile [g], Mulatie Mekonnen [a], Abebe D. Chukalla [h]

[a] Department of Natural Resource Management, College of Agriculture and Environmental Science, Bahir Dar University, Bahir Dar, Ethiopia
[b] College of Agriculture, Food and Natural Resources, Prairie View A&M University, Prairie View, TX, 77446, USA
[c] Wageningen University & Research, Water Resources Management Group, P.O. Box 47, 6700 AA, Wageningen, the Netherlands
[d] Kotebe University of Education, College of Business, Technology and Vocational Education, P.O. Box 31248, Addis Ababa, Ethiopia
[e] International Center for Agricultural Research in the Dry Areas (ICARDA), Addis Ababa, Ethiopia
[f] International Water Management Institute, Addis Ababa, Ethiopia
[g] College of Agriculture and Life Sciences, Texas A&M University, TX, USA
[h] The Department of Land and Water Management, IHE Delft Institute for Water Education, 2611 AX, Delft, the Netherlands
[i] Africa Center of Excellence for Climate-Smart Agriculture and Biodiversity Conservation, Haramaya University, Dire Dawa, Ethiopia

ARTICLE INFO

Keywords:
Groundwater
Pollution
Spatial analysis
Vulnerability
Modified DRASTIC

ABSTRACT

Groundwater is one of the most vital natural resources worldwide. However, shallow aquifers are prone to contamination, posing significant risks to human health, livestock, agricultural productivity, and economic growth. Identifying appropriate land management strategies is critical for mitigating groundwater vulnerability to pollution. This study evaluates groundwater vulnerability to pollution under various land management scenarios using the modified DRASTIC model in Bahir Dar City, Ethiopia. The analysis incorporates multiple parameters within the ArcGIS environment, including depth to water table, net recharge, aquifer characteristics, soil properties, topography, vadose zone, hydraulic conductivity, and land use/land cover (LULC). In this study, LULC was added as an additional parameter to enhance the DRASTIC model. Groundwater vulnerability to pollution was evaluated under four distinct land management scenarios: baseline, agricultural expansion, urbanization, and reforestation. A single-parameter sensitivity analysis and a map removal sensitivity analysis were performed to identify the most influential parameters affecting groundwater vulnerability under the baseline LULC conditions. The result revealed that groundwater vulnerability in Bahir Dar City under baseline conditions is primarily influenced by LULC and net recharge. The areal average groundwater vulnerability to pollution index at the baseline scenario was 184. Agricultural expansion and urbanization increased the areal average groundwater vulnerability to pollution by 4.9 % and 1.6 %, respectively, while the reforestation scenario reduced it by 1.6 %. These findings highlight the critical role of effective land management practices, such as reforestation, in mitigating groundwater susceptibility to pollution. The results also indicate that groundwater vulnerability to pollution

* Corresponding author. College of Agriculture, Food and Natural Resources, Prairie View A&M University, Prairie View, TX, 77446, USA.
E-mail address: gtemesgen114@gmail.com (T.G. Tarkegn).

https://doi.org/10.1016/j.heliyon.2025.e42660
Received 24 September 2024; Received in revised form 25 December 2024; Accepted 11 February 2025
Available online 12 February 2025

varies across different geological formations. Therefore, given the influence of geological variability on groundwater vulnerability, incorporating geological considerations into urban expansion planning is essential for minimizing the risk of groundwater contamination.

1. Introduction

Groundwater, which constitutes approximately 95 % of the available freshwater supply for humanity, is a vital resource for human life and economic development [1]. It serves as the primary water source for domestic and commercial uses, particularly in countries with limited surface water availability [1–4]. Over the past 50 years, global groundwater usage has significantly increased due to population growth, recurring droughts, its generally high quality, and the relatively low development cost [1]. In Africa, groundwater is the dominant source of drinking water, and its use for irrigation has grown substantially in recent decades. This trend is expected to persist due to factors such as population growth, urbanization, agricultural expansion, and planned irrigation developments aimed at enhancing food security [2,5,6].

To ensure the sustainable provision of clean groundwater for current and future generations, it is essential to manage this resource effectively by assessing and understanding its vulnerability to pollution [7,8]. Groundwater vulnerability assessment aims to protect this critical resource by identifying areas at risk of contamination and informing sustainable management practices [7,9]. The fundamental principle of such assessments is to classify areas into different vulnerability categories, which helps pinpoint the key factors contributing to groundwater pollution [10]. Providing vulnerability maps based on these assessments supports evidence-based decision-making and represents a crucial step toward sustainable groundwater and environmental management [6].

Bahir Dar City, the focus of this study, is one of Ethiopia's rapidly urbanizing centers. As in many other Ethiopian cities [11,12], groundwater serves as the primary source of domestic water supply [13]. However, groundwater quality in the City is under increasing pressure due to the disposal of pollutants, including septic tank effluents, landfill leachates, and industrial and domestic wastes, into both surface and groundwater bodies. Consequently, assessing the vulnerability of Bahir Dar's groundwater to pollution is critical for ensuring its sustainable management.

Previous studies, such as Alamne [13] have assessed groundwater vulnerability of Bahir Dar City using seven key parameters. However, their study excluded land use/land cover (LULC) - a critical factor that significantly influences groundwater vulnerability to pollution. Studies conducted both in Ethiopia [5,14] and globally [15] have demonstrated that LULC is among the most influential parameters affecting groundwater vulnerability. Moreover, prior research in Bahir Dar and other parts of Ethiopia [11,13,16] has not evaluated groundwater vulnerability under varying land management scenarios. In contrast, studies in other parts of the world, such as Sepehrara [17], have incorporated dynamic parameters and LULC changes to assess groundwater vulnerability comprehensively. Incorporating different land management scenarios is essential for understanding how various management options influence groundwater vulnerability, providing a basis for interventions to reduce contamination risks.

Additionally, the validation of groundwater vulnerability assessments in Ethiopia [11,13,16] has primarily relied on NO_3^- data alone. For a more comprehensive evaluation, it is essential to include other indicators, such as Total Dissolved Solids (TDS), which also significantly impact groundwater quality and its suitability for drinking purposes [7,12].

The main objective of this study is to evaluate the vulnerability of groundwater to pollution under different land management scenarios in Bahir Dar City, Ethiopia, using the modified DRASTIC model. The innovative aspects of this study include: 1)The

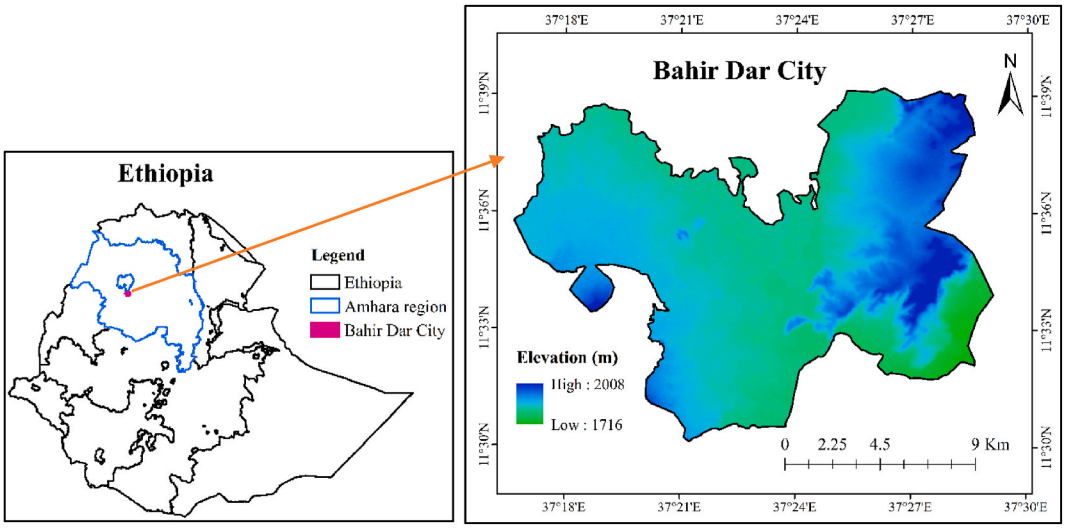

Fig. 1. Location of Bahir Dar City from Amhara region and Ethiopia.

application of the modified DRASTIC model, which integrates eight parameters for a more comprehensive assessment, 2) validation of the model using multiple data sources to enhance accuracy and reliability, and 3) evaluation of groundwater vulnerability under various land management scenarios (baseline, agricultural expansion, urbanization, and reforestation), providing insights into how different management practices influence groundwater susceptibility to pollution. By identifying the effects of land management options on groundwater vulnerability, this study offers valuable information for evidence-based decision-making and sustainable groundwater management. The findings will contribute to safeguarding groundwater resources and ensuring their long-term availability for domestic, agricultural, and economic uses.

2. Materials and methods

2.1. Study area

Bahir Dar City, covering an area of 21,341.8 ha, is situated in the Amhara region of Ethiopia, adjacent to Lake Tana. Geographically, the City lies between 11°30′ N-11°40′ N latitude and 37°15′ E−37°30′ E longitude (Fig. 1), with elevations ranging from 1716 to 2008 m above sea level (m a.s.l.). Based on data from the Ethiopian Meteorology Institute (EMI) and the Climate Hazards Group Infrared Precipitation with Stations, version 2.0 (CHIRPS v2.0), the long-term areal average annual rainfall of the City for the period 1990–2023 is approximately 1430 mm. The average temperature recorded at Bahir Dar station for the period 1992–2021 is 27.9 °C for the maximum and 11.9 °C for the minimum. The primary water supply sources for the City's residents include groundwater and springs, with limited contributions from Lake Tana [13]. The topography of the study area is predominantly flat; however, hills, rugged terrain, and undulating features are also observed in localized pockets. The region's climate is primarily influenced by the Inter-Tropical Convergence Zone (ITCZ), which drives two distinct seasons: a rainy season (June to September) and a dry season (October to May) [18].

The Northwestern Ethiopian Plateau, where Bahir Dar City is part of it, predominantly comprises Cenozoic rocks, including Tertiary trap (plateau) volcanics, minor Quaternary volcanics, and associated sedimentary deposits [19]. The Lake Tana sub-basin is underlain by tholeiitic Miocene-Pliocene basalts, supplemented by smaller amounts of felsites, nonmarine sedimentary rocks, and localized basaltic cinder cones and flows [20–22]. In the southern portion of the sub-basin, including the City of Bahir Dar, Quaternary scoriaceous basalts dominate the geological landscape [23].

Lake Tana and the majority of Bahir Dar City (77.9 %) (Fig. 2) are situated within volcanic centers formed at the convergence of three grabens: Dengel Ber (buried), Gondar (exposed by erosion), and Debre Tabor (reactivated) [24]. Termaber basalts, Alluvium deposits, and Ashangi basalts (Fig. 2) characterize about 21.1 % of the City. From the geological map of the City, approximately 1 % of the study area is occupied by sections of Lake Tana (Fig. 2). This geological framework indicates that groundwater sources in Bahir Dar City are primarily derived from local recharge and regional groundwater flow.

2.2. Descriptions of modified DRASTIC model

The modified DRASTIC model [25] is an enhanced version of the original DRASTIC model Aller [26] developed in the United States.

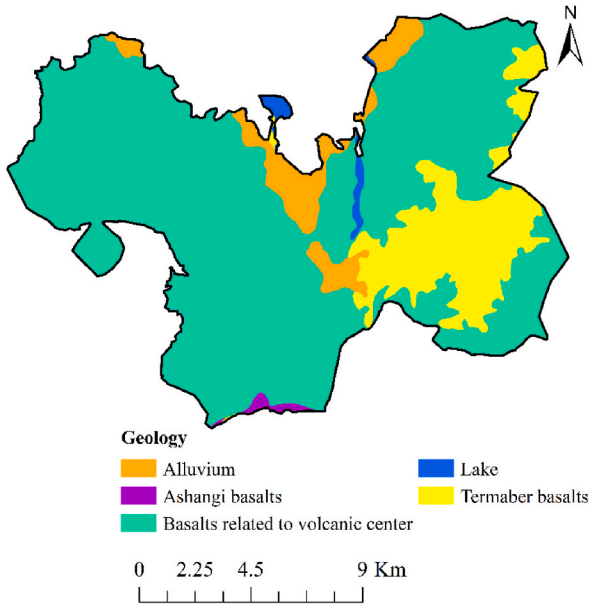

Fig. 2. The geological map of Bahir Dar City.

In this study, the modified DRASTIC model was employed to assess the groundwater vulnerability of Bahir Dar City to pollution. The model categorizes areas based on factors influencing groundwater contamination vulnerability.

While the original DRASTIC model incorporates seven physical parameters-Depth to water table, Recharge, Aquifer media, Soil media, Topography, Impact of the vadose zone, and Hydraulic conductivity [26]- the modified DRASTIC model includes an additional parameter, LULC, to account for human-induced changes [25]. The integration of LULC is critical because changes from vegetative cover to cultivated land or urban areas can introduce pollutant chemicals, which infiltrate groundwater or enter boreholes and springs through surface runoff.

Studies comparing the DRASTIC and modified DRASTIC models have consistently demonstrated the superior performance of the modified version in assessing groundwater vulnerability [16,27,28]. As a result, the modified DRASTIC model has been widely applied in groundwater studies both in Ethiopia [9,11,16] and globally [25,28–31].

2.3. Data types and sources for modified DRASTIC model

This study employed eight datasets to map groundwater vulnerability to pollution, building on methodologies used in previous studies conducted in Ethiopia [9,16] and internationally [25,27,28]. A detailed description of these datasets is presented below.

2.3.1. Depth to water table

Depth to the water table refers to the vertical distance between the ground surface and the water table [11]. In this study, the water

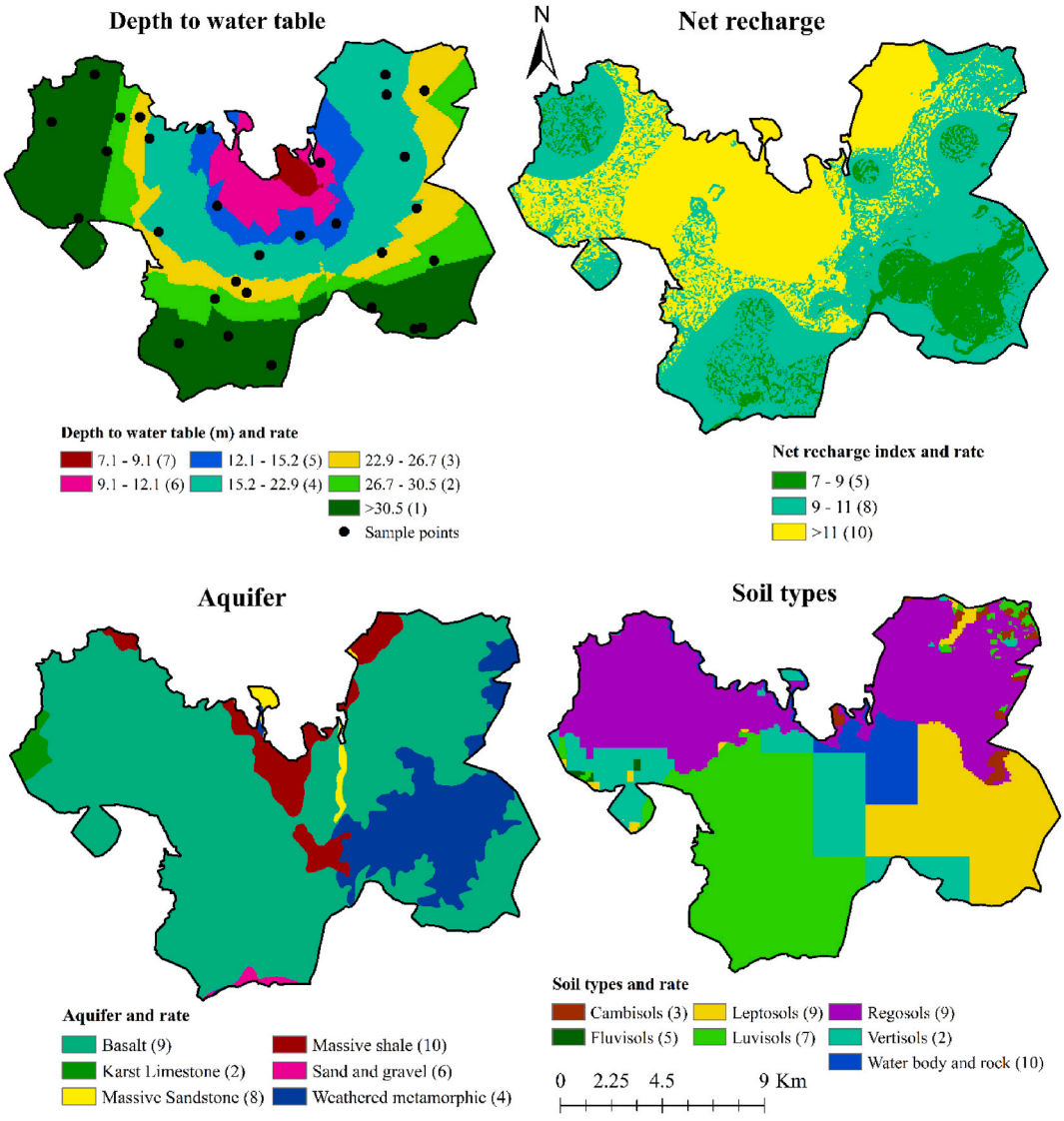

Fig. 3. The depth to the water table, net recharge, aquifer, and soil type maps of Bahir Dar City.

table depth data of 30 wells were obtained from the Amhara Design and Supervision Enterprise and the Bahir Dar City Water Supply and Sanitation Office. To transform the point data into a spatial representation (Fig. 3), the Kriging interpolation method was applied following literature [9,32,33]. This process enabled the generation of a continuous water table depth layer, which was subsequently reclassified into seven vulnerability classes (Table 1). The final reclassified water depth layer contains a 10 m spatial resolution.

The water table depths in the study area ranged from 7.12 to 42.91 m. Depths between 7.12 and 9.1 m were assigned a vulnerability rating of 7 (highest vulnerability), while depths exceeding 30.5 m were rated as class 1 (lowest vulnerability), as illustrated in Fig. 3. This classification reflects the general principle that groundwater vulnerability to pollution decrease with increasing water table depth.

The analysis revealed an average water table depth of 25.24 m across the study area. Of the 30 wells and springs surveyed, 31.4 % had depths exceeding 30.5 m, while only 1.3 % had depths less than 9.1 m (Table 2). The results clearly indicate that shallower water table depths significantly elevate the potential for pollution, with the shallowest depths receiving the highest vulnerability rankings.

2.3.2. *Net recharge*

Net recharge refers to the volume of surface water that infiltrates into the groundwater system [11,26]. Since net recharge data is not available for the study area, the study developed a net recharge index following Piscopo method [36], which requires rainfall, slope and soil permeability parameters. Due to the unavailability of net recharge data, the applied method was also implemented by several

Table 1
Parameters rate and weight classes of modified DRASTIC model.

Factor	Weight	Range	Rate	References
Depth to water table (m)	5	7.12–9.1	7	[3,14,26,29]
		9.1–12.1	6	
		12.1–15.2	5	
		15.2–22.9	4	
		22.9–26.7	3	
		26.7–30.5	2	
		>30.5	1	
Net recharge	4	7–9	5	[6,25]
		9–11	8	
		>11	10	
Aquifer	3	Massive shale	10	[14,26]
		Basalt	9	
		Massive sandstone	8	
		Sand and gravel	6	
		Weathered metamorphic	4	
		Karst limestone	2	
Soil	2	Waterbody and rock	10	[3,26,29]
		Regosol	9	
		Leptosol	9	
		Luvisol	7	
		Fluvisol	5	
		Cambisol	3	
		Vertisol	2	
Topography/slope (%)	1	0–2	10	[9,26]
		2–4	9	
		4–6	8	
		6–8	7	
		8–10	6	
		10–12	5	
		12–14	4	
		14–16	3	
		16–18	2	
		>18	1	
Vadose zone	5	Water body and rock	10	[26,34]
		Rubble	9	
		Loamy	5	
		Clay loam	3	
		Clay	1	
Hydraulic conductivity (m/day)	3	>39.71	10	[7,26]
		20.74–39.71	8	
		10.45–20.74	6	
		4.87–10.45	4	
		1.84–4.87	2	
		<1.84	1	
Land use land cover	5	Built-up area	10	[9,35,34]
		Cultivated land	9	
		Grassland	4	
		Water body	2	
		Forest	1	

Table 2
The coverage of depth to the water table and net recharge.

Depth to water table	Area in ha	Area in %	Net recharge	Area in ha	Area in %
7.12–9.1	285.6	1.3	7–9	2707.0	12.7
9.1–12.1	1340.5	6.3	9–11	10287.9	48.2
12.1–15.2	1585.6	7.4	>11	8346.9	39.1
15.2–22.9	5605.6	26.3	Total	21341.8	100
22.9–26.7	3021.4	14.2			
26.7–30.5	2794.4	13.1			
>30.5	6708.8	31.4			
Total	21341.8	100			

studies [6,25,37–39]. The detailed procedures for implementing Piscopo method [36] for developing a proxy to net recharge can be referred in Baki and Ghavami [6] and Moghaddam [39].

Rainfall data were collected from five meteorological stations-Bahir Dar, Zenzelema, Meshenti, Zege and Tis Abay-and were obtained from the Ethiopian Meteorology Institute (EMI). The mean annual rainfall data (1990–2023) for each station were computed and interpolated using the Kriging interpolation method [5] within a GIS environment. The Hydro-processing tools, such as SNAP Toolbox software, were used to derive the slope map from the Sentinel-1A Digital Elevation Model (DEM). With a 10-m spatial resolution, this DEM was sourced from the European Space Agency (ESA).

A soil type map of the study area was obtained from the Ministry of Water and Energy (MoWE), while soil properties for various soil types were gathered from the Harmonized World Soil Database (HWSD). Using the pedotransfer function, soil permeability for each soil type was derived based on soil texture data from the HWSD for three distinct soil layers. Due to the absence of required soil property data for many model-based studies, the pedotransfer method was widely used in the scientific community to estimate soil properties from textural data [40–42]. The derived soil permeability values for each soil type were subsequently converted into a raster format for further analysis.

The final net recharge index layer, which was converted to a 10 m spatial resolution, was reclassified into three sub-classes based on the values presented in Table 1. The study found that net recharge indexes within the City ranged from 7 to 14 (Fig. 3), with an average net recharge index of 11.09. Specifically, 48.2 % of the study area exhibited net recharge indexes between 9 and 11. In comparison, 39.1 % of the area experienced net recharge index exceeding 11 (Table 2 and Fig. 3). The remaining 12.7 % of the area had net recharge indexes between 7 and 9.

2.3.3. Aquifer

Aquifer media refer to geological formations that function as groundwater reservoirs, characterized by material properties that influence contaminant attenuation based on the permeability of each layer. The geological setting determines the aquifer's permeability and its ability to either restrict or permit the entry of pollutants into the groundwater [9]. According to the Ethiopian Geological Survey, the aquifer of Bahir Dar City is unconfined, featuring continuous permeable layers extending from the land surface to the base of the aquifer. It is typically recharged by rainwater or stream water infiltrating directly through the overlying soil. This study obtained aquifer media data in vector format from the Ethiopian Geological Survey. The attained aquifer media map of Bahir Dar City was transformed into a 10 m spatial resolution raster using a conversion tool, ensuring compatibility in spatial resolution and characteristics with other thematic layers.

The aquifer media data was then reclassified based on its sensitivity to contaminants, as shown in Table 1. The analysis revealed that 76.68 % of the City is primarily composed of basalt (Fig. 3 and Table 3), which received a sensitivity rate of 9 (Table 1). This composition indicates an elevated risk of groundwater pollution across most of the City's area.

2.3.4. Soil

Soil media refers to the upper layer of the subsoil, extending to the root zone of plants and regions of organic activity [11]. In this study, a soil type map was sourced from MoWE. The identified soil types include Liptosols, Regosols, Luvisols, Fluvisols, Vertisols, Cambisols, as well as water bodies and rock formations (Fig. 2). Following the methodology of Aller [26], the rate and weight of each soil type were assigned based on their relative significance and contribution to aquifer vulnerability. The soil data were subsequently

Table 3
Aquifer and soil type areal coverage of the study area.

Aquifer	Area in ha	Area in %	Soil type	Area in ha	Area in %
Massive shale	1325.9	6.21	Water body and rock	1144.04	5.36
Weathered metamorphic	3070.11	14.39	Regosols	7463.19	34.97
Massive sandstone	219.1	1.03	Leptosol	3847.45	18.03
Sand and gravel	101.7	0.48	Luvisol	5826.04	27.3
Basalt	16,364.01	76.68	Fluvisols	39.62	0.19
Karst limestone	260.97	1.22	Cambisols	277.86	1.3
Total	21,341.8	100	Vertisol	2743.61	12.86
			Total	21,341.8	100

classified into distinct categories based on sensitivity to contaminants (Table 1).

The analysis revealed the following distribution of soil types: Regosols occupy 34.97 %, and Luvisols account for 27.3 % of the area. In contrast, Vertisols cover 12.86 %, while Fluvisols and Cambisols are found in much smaller areas, covering 0.19 % and 1.3 %, respectively. In this area, the water body and rock cover 5.36 % (Fig. 3; Table 3). Consistent with other model parameters, the soil types were classified into varying vulnerability categories as detailed in Table 1, and then converted into a 10-resolution raster layer (Fig. 3).

2.3.5. *Topography*

Topography refers to the characteristics of the land surface, including features such as hills, plains, and mountains [11]. In the modified DRASTIC model, the slope map in percentage represents the topographic information. In this study, the slope map was developed from the 10-m spatial resolution Sentinel-1A DEM, which was obtained from the ESA. The resulting slope map was then reclassified following established literature (Table 1).

The analysis revealed that slope classes 1 and 2 were assigned ratings of 10 and 9, respectively, and together they account for 80.19 % of the total study area. Slopes greater than 18 % (steeper slopes), specifically those between 16 % and 18 %, cover 2.63 % of the area, as shown in Fig. 4 and Table 4. Regarding slope, these findings indicate that the majority of the study area is highly susceptible to pollution.

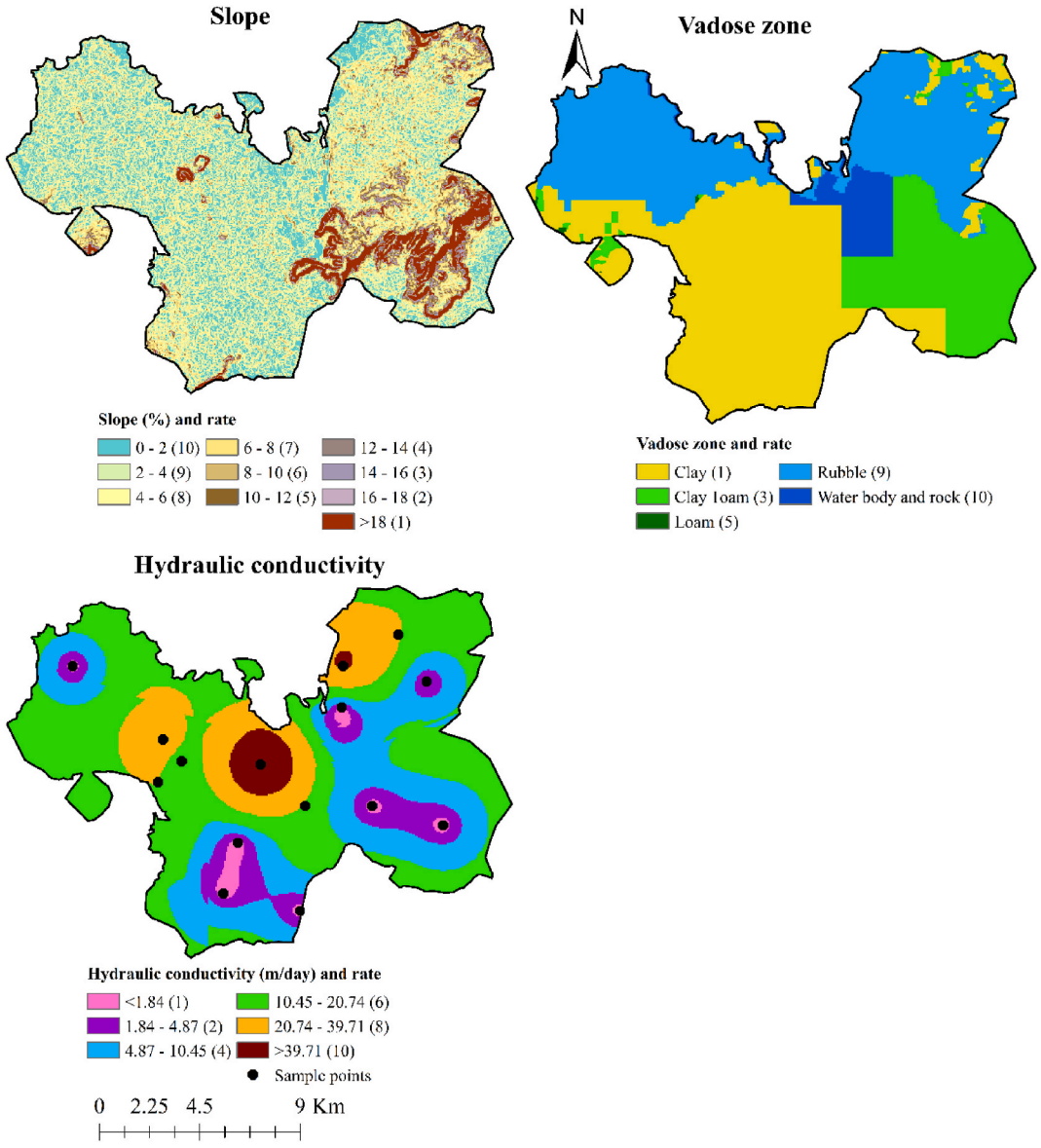

Fig. 4. The slope, vadose zone, and hydraulic conductivity of the study area.

Table 4
The slope, vadose zone, and hydraulic conductivity area coverage of the City.

Slope class	Area in ha	Area in %	Vadose zone	Area in ha	Area in %	Hydraulic conductivity	Area in ha	Area in %
0–2	10,018.28	46.94	Water body and rock	1144.31	5.36	<1.84	373	1.7
2–4	7095.21	33.25	Rubble	7461.58	34.96	1.84–4.87	1791.4	8.4
4–6	1643.53	7.7	Loamy	23.01	0.11	4.87–10.45	5447.3	25.5
6–8	735.82	3.45	Clay loam	3935.02	18.44	10.45–20.74	9785.5	45.9
8–10	477	2.24	Clay	8777.88	41.13	20.74–39.71	3221.2	15.1
10–12	334.85	1.57	Total	21,341.8	100	>39.71	723.5	3.4
12–14	264.3	1.24				Total	21,341.8	100
14–16	212.29	0.99						
16–18	176.97	0.83						
>18	383.57	1.8						
Total	21,341.8	100						

2.3.6. *Vadose zone*

The vadose zone refers to the unsaturated area situated below the soil horizon and above the water table [9,26]. The influence of the vadose zone was assessed based on the distribution of soil texture and its characteristics, which were sourced from the Amhara National Regional State Bureau of Environmental Protection. The soil texture rates were determined based on particle size and composition. These characteristics were then used to evaluate the impact of the vadose zone, with ratings assigned based on the criteria outlined in Table 1. Subsequently, the developed vadose zone data were converted into a raster layer (10 m resolution) (Fig. 4).

The study area mainly comprises clay and rubble soils, covering 41.13 % and 34.96 %, respectively. The remaining area includes loamy soil, clay loam, water bodies, and rock, which collectively account for 23.91 % of the total area (Fig. 4 and Table 4).

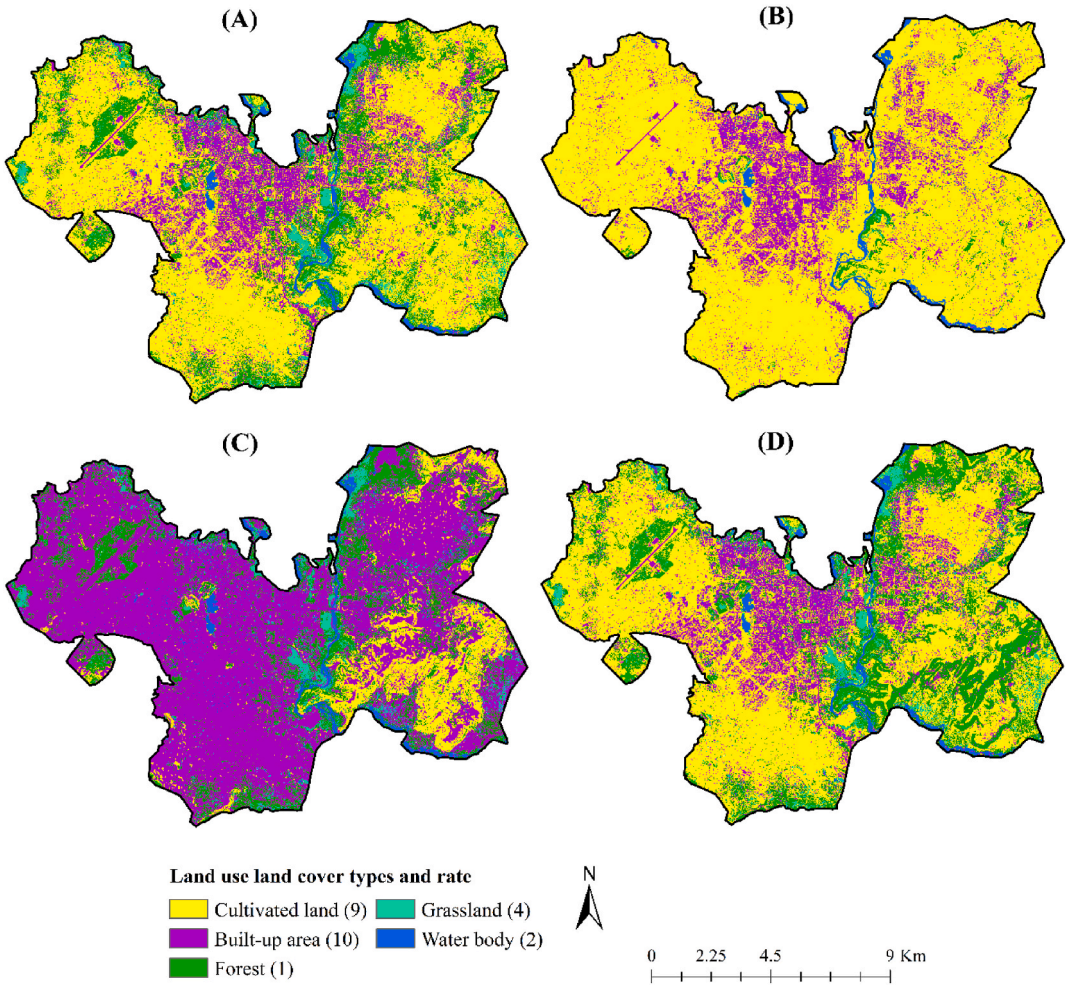

Fig. 5. The LULC type maps of the study area at the baseline (A), agricultural expansion (B), urbanization (C) and reforestation (D) scenarios.

2.3.7. Hydraulic conductivity

Hydraulic conductivity refers to the ability of aquifer materials to transmit water, thereby determining groundwater flow rates under a given hydraulic gradient [11,26]. In this study, hydraulic conductivity data were generated from 15 wells (Fig. 4). A point feature shape file was created, and Kriging interpolation method [5,32,33] was applied to generate a continuous hydraulic conductivity surface across the study area. The resulting hydraulic conductivity layer was then classified according to established literature (Table 1). Therefater, the classified map was converted to a 10 m spatial resolution layer to match with the characteristics of other model inputs (Fig. 4).

The hydraulic conductivity values in the study area range from 0.115 to 71.5 m/day, with six distinct classes, as shown in Fig. 4. The results reveal that 45.9 % of the study area exhibits conductivity values between 10.45 and 20.74 m/day, while 25.5 % falls within the range of 4.87–10.45 m/day (Table 4). An additional 15.1 % of the area has conductivity values between 20.74 and 39.71 m/day, and 3.4 % shows values greater than 39.71 m/day. The remaining 10.1 % of the study area has hydraulic conductivity values below 4.87 m/day, as detailed in Table 4.

2.3.8. Land use land cover

LULC represents both the physical characteristics of the land surface and its human utilization. To create the LULC map, a Sentinel-2 MSI Level-1C image from February 2023 was acquired from the Copernicus hub. Sentinel-2 provides high radiometric, spatial, spectral, and temporal resolution, making it ideal for LULC analysis.

A supervised image classification method, utilizing 250 sample points, was employed to classify the satellite image into LULC classes. The final LULC map of Bahir Dar City, with a 10 m resolution, contains five primary classes: built-up area, cultivated land, grassland, forest, and water bodies. To ensure accuracy, an assessment was performed using 100 reference points collected from field surveys and Google Earth imagery.

The overall Kappa coefficient for classification was 0.814 (81.4 %), and the accuracy assessment yielded a coefficient of 0.83 (83 %), both of which are considered acceptable [43]. The generated LULC map, which represents the baseline scenario in Fig. 5 and Table 5, was then reclassified based on the criteria outlined in Table 1. The classification results revealed that cultivated land covers 60.75 % of the study area, while forest accounts for 17.27 % and built-up areas comprise 14.72 %. Grassland and water bodies cover the remaining area, as shown in Fig. 5 and Table 5.

2.4. Rate and weight of parameters for the model

As discussed in section 2.3 and outlined in Table 1, each parameter used in the modified DRASTIC model was rated on a scale from 1 to 10. Higher values represent the most vulnerable subclasses to groundwater pollution, while lower values indicate the least susceptible subclasses. In addition, weights were assigned to the eight parameters, ranging from 1 to 5, based on established literature (Table 1). A weight of 5 corresponds to the most significant parameters in relation to groundwater pollution, while a weight of 1 denotes the least significant parameters [30].

2.5. Vulnerability index and vulnerability classes

Groundwater vulnerability was evaluated after preparing the thematic layers for each parameter based on their respective ranges as well as projection of all output rasters to WGS 1984 UTM Zone 37N reference system. The resulting vulnerability index, derived from the modified DRASTIC model, was then reclassified into various vulnerability levels, as shown in Table 6, following the methodology outlined in the literature [9,26].

The vulnerability categories indicate the degree of protection needed for groundwater conservation. Areas classified as very high or highly vulnerable require the most stringent protection, as they are highly susceptible to a wide range of water pollutants and are considered maximum protection zones. Areas with moderate vulnerability are at risk from certain pollutants and are identified as requiring high levels of protection [44].

2.6. Model validation

Although groundwater can be contaminated by various physicochemical and biological pollutants, the concentrations of NO_3^- and

Table 5
The LULC type areal coverage at the baseline, agricultural expansion, urbanization and reforestation scenarios.

LULC type	Baseline		Agricultural expansion		Urbanization		Reforestation	
	Area in ha	Area in %	Area in ha	Area in %	Area in ha	Area in %	Area in ha	Area in %
Built-up area	3141.2	14.72	3159.1	14.8	13561.4	63.5	3166.2	14.8
Forest	3685.41	17.27	312.0	1.5	3713.5	17.4	4840.1	22.7
Water body	717.88	3.36	738.4	3.5	746.0	3.5	745.5	3.5
Cultivated land	12,965.3	60.75	17079.7	80.0	2460.8	11.5	11730.3	55.0
Grassland	832.01	3.9	52.6	0.2	860.1	4.0	859.7	4.0
Total	21,341.8	100	21,341.8	100	21,341.8	100	21,341.8	100

Table 6
The vulnerability categories in the applied model.

Vulnerability category	Very low	Low	Moderate	High	Very high
Vulnerability index score	<100	100–145	145–190	190–235	>235

TDS are among the most common and significant in terms of their impact on water quality and human health. As a result, these parameters are frequently used to validate groundwater vulnerability assessments [9,11].

In our study, water samples were collected from 15 wells, chosen explicitly from areas with varying levels of vulnerability: very high (4 samples), high (4 samples), moderate (4 samples), and low (3 samples). The samples were taken after 6–10 min of pumping to ensure consistent water flow. The water was collected in clean plastic bottles, stored in a cold box, and transported to the North Wollo Zone Water and Energy Laboratory within 48 h for analysis. In this study, Pearson's correlation coefficient method was employed to assess the relationships between the concentrations of NO_3^- and TDS with the groundwater vulnerability following previous studies [6,7,16]. Before conducting the correlation analysis, a normality assessment was performed using the Shapiro-Wilk test [45,46] to determine whether the datasets followed a normal distribution.

2.7. Sensitivity analysis

Sensitivity analysis is a method used to identify the most influential parameters that affect the vulnerability of groundwater to pollution, thereby informing effective groundwater management strategies [9,35]. In this study, two renewed sensitivity analysis methods were employed: single parameter sensitivity analysis and map removal sensitivity analysis [4,9,16,27,30].

Single parameter sensitivity analysis helps identify the most sensitive parameters within the analytical model. On the other hand, map removal sensitivity analysis assesses the impact of each parameter on the vulnerability index by systematically removing one parameter at a time [16,35]. The comparison is then made between the vulnerability index obtained after removing the parameter and the original index (which includes all parameters) to evaluate the influence of each parameter on the overall model. Both sensitivity analysis methods have been successfully applied in recent studies [9,11,35].

2.8. Land management scenarios

This study considered four land management scenarios: baseline, agricultural expansion, urbanization, and reforestation. The baseline scenario represents the current LULC and land management conditions, classified from the 2023 Sentinel Image. The agricultural expansion and urbanization scenarios were selected based on widely reported projections of future LULC changes, such as the expansion of cultivated lands and urban areas, as documented in previous studies in Ethiopia [47,48]. The reforestation scenario was chosen in response to ongoing land rehabilitation efforts and tree planting campaigns across Ethiopia [49]. The detailed descriptions of these land management scenarios, along with the rationale for their selection, are provided below.

The agricultural expansion scenario suggests that increasing cultivated lands will satisfy the food demands of a growing population. To mitigate land degradation associated with this expansion, it is assumed that cultivated lands will be confined to areas with slope of less than 15 % [50]. This scenario is based on the assumption that future agricultural expansion in the study region, and Ethiopia as a whole, will primarily occur at the expense of vegetative LULC types, such as grasslands and forests, particularly in areas with slopes below 15 % [47,48].

The urbanization scenario predicts the expansion of built-up areas, which, according to previous studies, typically occurs at the expense of cultivated lands in the study region and Ethiopia at large [47,48]. In this scenario, cultivated lands with slopes below 8 % are converted to urban areas.

The reforestation scenario aims to combat land degradation by restricting cultivation in areas with slopes greater than 15 % [40,50]. In this scenario, cultivated lands on slopes greater than 15 % are converted to forested areas to promote land recovery. The LULC maps and the areal coverage for each category of the four land management scenarios are provided in Fig. 5 and Table 5.

2.9. Methods of evaluating the vulnerability of groundwater to pollution under different land management scenarios

This study assessed groundwater vulnerability to pollution under four land management scenarios such as baseline, agricultural expansion, urbanization and reforestation. The approach used in this study involved modifying the LULC inputs while keeping all other model parameters constant, in line with methods applied in previous research on similar [17] and other environmental topics [40–42,50].

3. Results and discussion

3.1. Model validation

Based on laboratory tests conducted on samples collected from 15 wells, the groundwater quality analysis revealed that NO_3^- and TDS values ranged from 1.9 to 13.1 mg/L and 78.8–498 mg/L, respectively (Fig. 6). The mean values for these parameters were

determined as 6.64 mg/L for NO_3^- and 250.13 mg/L for TDS.

Previous studies in the same and similar study areas have reported varying results regarding correlation coefficients. For instance, Alamne [13] investigated groundwater vulnerability in Bahir Dar City and reported a correlation coefficient of 0.53 for NO_3^-. The higher correlation coefficient observed in this study can be attributed to the enhanced method employed for estimating net recharge, incorporating variables such as rainfall, slope, and soil permeability, instead of relying solely on rainfall, as in Alamne [13]. Additional discrepancies in correlation coefficients may stem from differences in the modified DRASTIC model inputs as well as the inclusion of LULC parameter in this study.

Nevertheless, Abera [11] study in Mekelle City reported correlation coefficients of 0.681 and 0.702 for NO_3^- using the DRASTIC and modified DRASTIC models, respectively. Other studies conducted in Ethiopia [16] and globally [6,7,30,31] also reported NO_3^- correlation coefficients exceeding 0.50. Conversely, lower correlation coefficients (<0.5) have been observed in some global studies, such as Moghaddam, Nouri Sangarab [25]. The variations in the strength of correlation coefficients may result from differences in the quality of input data, the methodologies employed in model calibration, and the accuracy of the measured data used for model validation. Consistent with the TDS correlation coefficient reported in this study, other global studies have also documented values exceeding 0.5 [7].

The distribution of NO_3^- and TDS concentrations across different geological formations in the study area is summarized in Table 7. Four statistical measures-minimum, maximum, mean, and standard deviation-were used to evaluate whether specific geological types exhibited the highest or lowest concentrations of NO_3^- and TDS. The findings reveal that Alluvium and Basalts associated with volcanic centers showed the highest maximum, mean, and standard deviation values for both NO_3^- and TDS (Table 7), indicating their susceptibility to elevated concentrations. Termaber Basalts emerged as the third most vulnerable formation, ranking high in terms of minimum, maximum, and standard deviation for NO_3^- and TDS, suggesting these aquifers face significant risks (Table 7). In contrast, Ashangi Basalts consistently displayed the lowest maximum and standard deviation values, indicating a relatively lower degree of contamination and variability.

However, the lowest minimum and mean concentrations were observed in Basalts related to volcanic centers and Termaber Basalts, respectively, suggesting spatial heterogeneity in contamination levels even within vulnerable formations. These findings underscore the prominent role of geological characteristics in influencing NO_3^- and TDS concentrations. The elevated levels in Alluvium and Basalts associated with volcanic centers may be linked to their lithological properties, such as high porosity and permeability, coupled with proximity to contamination sources. Conversely, the lower concentrations in Ashangi Basalts may reflect limited permeability or reduced exposure to pollutant sources. These insights highlight the need for targeted management strategies, particularly for formations with higher vulnerability, to mitigate risks to water quality and safeguard these vital aquifers.

3.2. Sensitivity analysis

The sensitivity analysis using the single-parameter sensitivity method revealed that the effective weights of LULC (22.97 %) and net recharge (22.56 %) exceeded their theoretical weights of 17.86 % and 14.29 %, respectively (Table 8). This indicates that LULC and net recharge have a more considerable impact on groundwater vulnerability than other parameters, such as the vadose zone media and depth to the groundwater table, which demonstrated effective weights of 14.97 % and 13.31 %, respectively (Table 8).

Further insights were provided by the map removal sensitivity analysis, which also identified LULC and net recharge as the most sensitive parameters affecting groundwater vulnerability in Bahir Dar City (Table 9). The average vulnerability indices, calculated after sequentially removing thematic layers of LULC, net recharge, aquifer media, vadose zone, hydraulic conductivity, depth to the water table, soil, and topography were 129, 141, 152, 142, 151, 149, 162, and 175, respectively-values consistently below the overall

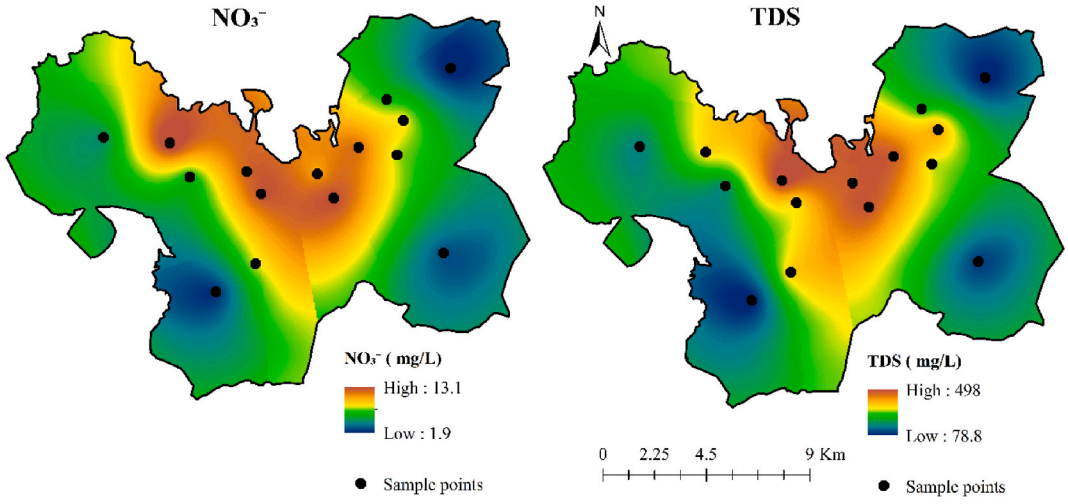

Fig. 6. The concentration of NO_3^- and TDS in Bahir Dar City.

Table 7
The concentrations of NO_3^- and TDS in different geological types of the study area.

Geology	NO_3^-				TDS			
	Min	Max	Mean	SD	Min	Max	Mean	SD
Alluvium	5.08	11.78	9.5	2.05	176.49	496	358.06	88.52
Ashangi basalts	5.34	7.11	5.93	0.54	209.15	273.17	229.78	20.65
Basalts related to volcanic center	1.92	13.06	6.57	2.4	78.83	497.97	245.24	85.35
Termaber basalts	2.43	11.11	5.55	1.92	109.04	462.9	218.26	69.16

Table 8
The sensitivity of parameters based on the single parameter sensitivity method.

Parameter	Theoretical weight	Theoretical weight (%)	Effective weight (%)		
			Max	Mean	Min
Depth of water table	5	17.86	16.26	13.31	7.57
Recharge	4	14.29	16.33	22.56	52.18
Aquifer	3	10.71	12.35	10.78	9.23
Soil	2	7.14	8.23	7.19	6.15
Topography	1	3.57	4.22	3.37	1.42
Vadose zone	5	17.86	18.52	14.97	7.69
Hydrologic conductivity	3	10.71	12.51	9.97	4.81
LULC	5	17.86	26.9	22.97	55.75

mean vulnerability index of 184. The sensitivity index values further confirmed the prominent influence of LULC and net recharge, with differences of 54 and 42, respectively, followed by the vadose zone (41) and depth to the water table (34). Both sensitivity analysis methods consistently highlighted LULC and net recharge as the dominant factors influencing groundwater vulnerability to pollution.

The pronounced role of LULC and net recharge in influencing groundwater vulnerability in our study aligns with previous studies. For example, a study by Asmamaw and Debie [5] in the same study area identified LULC as a key factor affecting groundwater quality. Similarly, Asfaw and Mengistu [9] reported that LULC and net recharge were the most influential parameters affecting groundwater vulnerability in the Megech watershed. Other studies conducted in Ethiopia have also emphasized the impact of anthropogenic activities, including LULC, as primary drivers of groundwater pollution [11,16]. Globally, studies by Al-Rawabdeh [34] and Shirazi [3] have further corroborated the significant role of human-induced factors in groundwater pollution.

In this study, the vadose zone and water table depth were also found to have significant impact on groundwater vulnerability. This finding aligns with results from Zenebe [16], who identified the vadose zone and water table depth as significant factors in the Elalla-Aynalem catchment, Ethiopia. Similarly, a study in Greece by Kazakis and Voudouris [15] demonstrated the influence of the vadose zone, aquifer media, and LULC on groundwater pollution.

Conversely, other studies conducted in numerous areas of the globe have also reported differing factors as predominant. For instance, Moghaddam [25] in the Ajabshir Plain, Iran, and Huan [51] in Jilin City, China, found hydrological conductivity and soil to be key drivers of groundwater vulnerability. Other studies have identified net recharge [30,35,52] and slope [52] as influential factors. These discrepancies can be attributed to variations in geological and hydrological characteristics, disparities in land management practices as well as varying extent of industrial and agricultural activities across study areas.

3.3. Vulnerability of groundwater to pollution under different land management scenarios

The vulnerability of groundwater to pollution under baseline conditions, as well as scenarios involving agricultural expansion, reforestation, and urbanization, is summarized in Table 10 and illustrated in Fig. 7. The results indicate that the total vulnerability

Table 9
The sensitivity of parameters according to the map removal method.

Parameter	Vulnerability index				Sensitivity index			
	Max	Mean	Min	SD	Max	Mean	Min	SD
Depth of water table	225	149	54	32.4	49	34	15	3.9
Recharge	223	141	49	33.2	51	42	20	3.1
Aquifer	242	152	55	33.6	32	31	14	2.7
Soil	248	162	63	33.5	26	21	6	2.8
Topography	262	175	64	35.1	12	8	5	1.2
Vadose zone	229	142	51	32.9	45	41	18	3.4
Hydrologic conductivity	235	151	53	32.5	39	32	16	3.8
LULC	203	129	51	29.8	71	54	18	6.5

values across the study area under these scenarios range from 69 to 274. As outlined in Section 2.5, these vulnerability indices are categorized into five classes: very low, low, moderate, high, and very high (Fig. 7, Table 10).

Under the baseline scenario, the average groundwater vulnerability value for the study area is 184. In this scenario, 43.7 %, 32.1 %, and 9.7 % of the area fall into the moderate, high, and very high vulnerability classes, respectively (Table 10). Zones of low and very low vulnerability account for approximately 13.5 % and 1 % of the study area, respectively.

Consistent with the substantial proportion (85.5 %) of the study area classified as having moderate to very high groundwater vulnerability under the baseline scenario, previous studies conducted in similar regions in Ethiopia have reported comparable findings [9,11,13]. For example, Alamne [13] observed that 70 % of Bahir Dar City is vulnerable to moderate to very high groundwater pollution. Similarly, Asfaw and Mengistu [9] reported that over 85 % of the Megech watershed falls within the moderate to very high vulnerability classes. Other studies in Ethiopia, such as those by Zenebe [16] in the Elalla-Aynalem catchment and Abera [11] in Mekelle City, also found that a significant proportion of study sites were categorized within the moderate to very high vulnerability classes.

The groundwater vulnerability under the baseline scenario was further analyzed with respect to the geological formations of the study area (Table 11). Statistical measures, including minimum, maximum, mean, and standard deviation, were employed to determine the geological formations exhibiting the highest and lowest levels of groundwater vulnerability. The analysis revealed that the Alluvium and Basalts related to volcanic centers demonstrated the highest maximum, mean, and standard deviation values, indicating a greater vulnerability to groundwater pollution. In contrast, the lowest values for these statistics were recorded in the Ashangi Basalts, reflecting their reduced vulnerability to groundwater pollution. The Termaber Basalts exhibited the third-highest values for maximum, mean, and standard deviation, highlighting this aquifer's susceptibility to groundwater pollution. Overall, Alluvium and Basalts related to volcanic centers emerged as the most vulnerable geological units to groundwater contamination, while the Ashangi Basalts generally demonstrated the lowest vulnerability across most statistical measures (Table 11).

Under the agricultural expansion scenario, the areal average groundwater vulnerability index increased to 193, representing a 4.9 % rise in mean vulnerability compared to the baseline scenario. In this scenario, 42.6 %, 37.9 %, and 12.7 % of the study area fall into the moderate, high, and very high vulnerability categories, respectively, while the low and very low categories account for 6 % and 0.8 %, respectively (Table 10). The implementation of the agricultural expansion scenario led to a significant increase in areas classified as high and very high vulnerability, with coverage expanding by 18 % and 30.8 %, respectively. Conversely, this scenario reduced areas classified as very low, low, and moderate vulnerability by 27.4 %, 55.1 %, and 2.4 %, respectively.

The implementation of the urbanization scenario increased the average groundwater vulnerability index to 187, reflecting a 1.6 % rise in mean groundwater pollution compared to the baseline scenario. The results indicate that 42 % of the study area falls within the moderate vulnerability zone, 33 % within the high vulnerability zone, and 11.5 % within the very high vulnerability zone. Additionally, 12.5 % of the area is categorized as low vulnerability, while 1 % is classified as very low (Table 10). Under the urbanization scenario, the coverage of very low, low, and moderate vulnerability zones decreased by 3 %, 7.5 %, and 3.9 %, respectively. In contrast, the areas classified as high and very high vulnerability increased by 2.8 % and 18.9 %, respectively.

Under the reforestation scenario, the mean groundwater vulnerability index decreased to 181, representing a 1.6 % reduction in the areal average vulnerability to pollution. The results indicate that 3.8 % and 14.2 % of the study area fall within the very low and low vulnerability zones, respectively (Table 10). The moderate, high, and very high vulnerability classes account for 40.6 %, 31.8 %, and 9.6 % of the area, respectively (Table 10). The implementation of the reforestation scenario resulted in significant increases in the coverage of very low and low vulnerability zones by 262.8 % and 5.5 %, respectively. Conversely, the areas classified as moderate, high, and very high vulnerability decreased by 7.1 %, 1.1 %, and 0.8 %, respectively (Table 10; Fig. 7).

Overall, changes in LULC to agricultural and urban uses have increased groundwater vulnerability to pollution, while the reforestation scenario contributed to a reduction in groundwater vulnerability. Consistent with these findings, previous studies in the same study area indicated that LULC is a key factor influencing groundwater quality [13]. The study by Sepehrara et al. (2023) in the Hashtgerd Plain, Iran, also demonstrated that projected expansions in agricultural and built-up areas significantly impacted groundwater vulnerability. Similarly, LULC has been identified as a critical parameter for groundwater vulnerability to pollution in several studies conducted in Ethiopia [9,11,16] and elsewhere in the world [3,15,53]. Additionally, agricultural practices and sewage disposal in urban areas have been recognized as major contributors to groundwater pollution in India [54,55].

Table 10
Areal distribution of groundwater vulnerability classes across the study area under baseline, agricultural expansion, urbanization, and reforestation scenarios.

Vulnerability class	Vulnerability index	Baseline		Agricultural expansion		Urbanization		Reforestation	
		Area in ha	Area in %	Area in ha	Area in %	Area in ha	Area in %	Area in ha	Area in %
Very low	<100	226.2	1	164.3	0.8	219.5	1	820.7	3.8
Low	100–145	2874	13.5	1290.1	6	2657.2	12.5	3031.6	14.2
Moderate	145–190	9320.1	43.7	9097	42.6	8960.8	42	8659.3	40.6
High	190–235	6856	32.1	8088.5	37.9	7047.9	33	6782.1	31.8
Very high	>235	2065.5	9.7	2702	12.7	2456.4	11.5	2048.1	9.6
Total		21,341.8	100	21,341.8	100	21,341.8	100	21,341.8	100

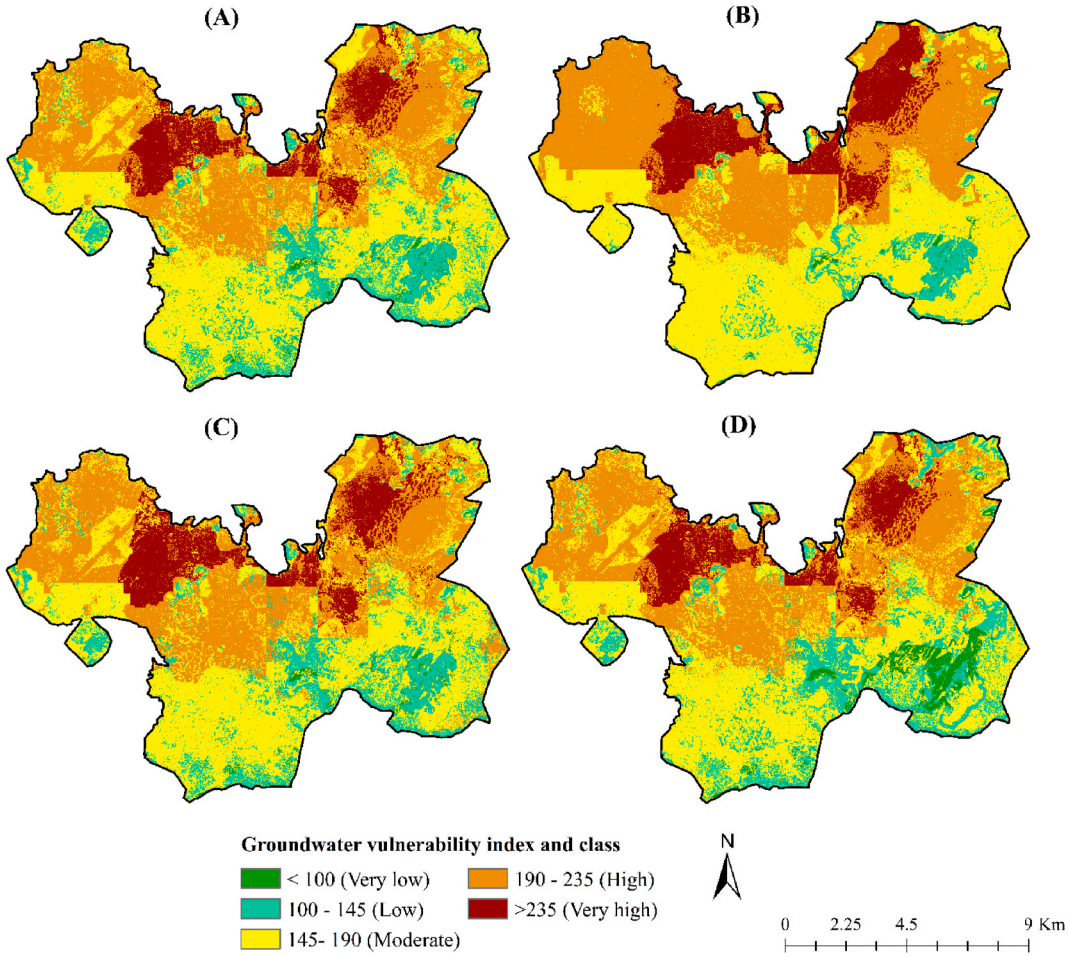

Fig. 7. The groundwater vulnerability to pollution of Bahir Dar City at the baseline, agricultural expansion, urbanization and reforestation scenarios.

Table 11
Groundwater vulnerability indices across different geological formations under the baseline LULC conditions of the study area.

Geology	Groundwater vulnerability index			
	Min	Max	Mean	SD
Alluvium	93	274	179.91	36.96
Ashangi basalts	95	174	128.57	21.22
Basalts related to volcanic center	84	274	188.98	35.34
Termaber basalts	69	254	157.41	27.56

4. Conclusion

This study evaluated the vulnerability of groundwater to pollution under four distinct land management scenarios using the modified DRASTIC model in Bahir Dar City, Ethiopia. The scenarios examined included the baseline, agricultural expansion, urbanization, and reforestation scenarios. Single-parameter sensitivity analysis and map removal sensitivity analysis were employed to identify the most influential parameters affecting groundwater vulnerability to pollution under the baseline LULC conditions. The findings reveal that LULC and net recharge are the most significant factors influencing groundwater vulnerability to pollution under the baseline scenario, with an average groundwater vulnerability index of 184. In the agricultural expansion and urbanization scenarios, the average groundwater vulnerability index increased by 4.9 % and 1.6 %, respectively.

In contrast, the reforestation scenario reduced the average vulnerability index by 1.6 %. These results indicate that agricultural expansion and urbanization exacerbate groundwater susceptibility to pollution, while reforestation serves as an effective mitigation strategy. Therefore, the study emphasizes the critical need for sustainable land management practices, such as reforestation, to

mitigate groundwater contamination and protect long-term water resources. The finding also showed that the vulnerability of groundwater to pollution varies within geological formations. Consequently, incorporating geological considerations into future urban expansion plans could further reduce groundwater vulnerability.

CRediT authorship contribution statement

Wasie Asmamaw Ashagrie: Writing – review & editing, Writing – original draft, Software, Methodology, Data curation, Conceptualization. **Temesgen Gashaw Tarkegn:** Writing – review & editing, Writing – original draft, Visualization, Supervision, Software, Methodology, Data curation, Conceptualization. **Ram Lakhan Ray:** Writing – review & editing, Writing – original draft. **Gebrekidan Worku Tefera:** Writing – review & editing, Writing – original draft. **Sintayehu Fetene Demessie:** Writing – review & editing, Writing – original draft. **Lewoye Tsegaye:** Writing – review & editing, Writing – original draft. **Anwar Assefa Adem:** Writing – review & editing, Writing – original draft. **Abeyou W. Worqlul:** Writing – review & editing, Writing – original draft. **Pieter R. van Oel:** Writing – review & editing, Writing – original draft. **Enyew Adgo:** Writing – review & editing, Writing – original draft. **Amare Haileslassie:** Writing – review & editing. **Yihun T. Dile:** Writing – review & editing. **Mulatie Mekonnen:** Writing – review & editing, Writing – original draft. **Abebe D. Chukalla:** Writing – review & editing, Writing – original draft.

Data availability statement

Data are available upon reasonable request.

Funding

This study did not receive financial support.

Declaration of competing interest

The authors declare no competing interests.

Acknowledgement

The data utilized in this study were sourced from the Amhara Design and Supervision Enterprise, Bahir Dar City Water Supply and Sanitation Office, Ethiopian Meteorology Institute, Ethiopian Geological Survey, Amhara National Regional State Bureau of Environmental Protection, Ministry of Water and Energy, Harmonized World Soil Database, and the European Space Agency. Laboratory analyses of the collected samples were conducted at the North Wollo Zone Water and Energy Laboratory. The revisions of the manuscript were performed during the corresponding author's Postdoctoral stay at Prairie View A&M University, Texas, USA. The authors sincerely thank these institutions and offices for their support. The authors also thank the journal's editor and the four anonymous reviewers for their insightful and constructive feedback.

References

[1] S. Foster, et al., Groundwater—a global focus on the 'local resource', Curr. Opin. Environ. Sustain. 5 (6) (2013) 685–695.
[2] S. Adelana, A. MacDonald, Applied Groundwater Studies in Africa: IAH Selected 599 Papers on Hydrogeology, vol. 13, 2008.
[3] S.M. Shirazi, H.M. Imran, S. Akib, GIS-based DRASTIC method for groundwater vulnerability assessment: a review, J. Risk Res. 15 (8) (2012) 991–1011.
[4] Y. Abduljaleel, et al., Enhancing groundwater vulnerability assessment for improved environmental management: addressing a critical environmental concern, Environ. Sci. Pollut. Control Ser. 31 (13) (2024) 19185–19205.
[5] M. Asmamaw, E. Debie, Characterizing groundwater quality for a safe supply of water using WQI and GIS in Bahir Dar city, northwest Ethiopia, Water Pract. Technol. 18 (4) (2023) 859–883.
[6] A.M. Baki, S.M. Ghavami, A modified DRASTIC model for groundwater vulnerability assessment using connecting path and analytic hierarchy process methods, Environ. Sci. Pollut. Res. Int. 30 (51) (2023) 111270–111283.
[7] A. Bera, et al., Groundwater vulnerability assessment using GIS-based DRASTIC model in Nangasai River Basin, India with special emphasis on agricultural contamination, Ecotoxicol. Environ. Saf. 214 (2021) 112085.
[8] A.R. Dizaji, et al., Groundwater contamination vulnerability assessment using DRASTIC method, GSA, and uncertainty analysis, Arabian J. Geosci. 13 (14) (2020).
[9] D. Asfaw, D. Mengistu, Modeling megech watershed aquifer vulnerability to pollution using modified DRASTIC model for sustainable groundwater management, Northwestern Ethiopia, Groundwater Sustain. Dev. 11 (2020).
[10] M. Sarkar, S.C. Pal, Application of DRASTIC and modified DRASTIC models for modeling groundwater vulnerability of Malda district in West Bengal, J. Indian Soc. Remote Sens. 49 (5) (2021) 1201–1219.
[11] K.A. Abera, et al., Vulnerability mapping of groundwater resources of Mekelle city and surroundings, Tigray region, Ethiopia, Water 14 (16) (2022).
[12] T.T. Aragaw, G. Gnanachandrasamy, Evaluation of groundwater quality for drinking and irrigation purposes using GIS-based water quality index in urban area of Abaya-Chemo sub-basin of Great Rift Valley, Ethiopia, Appl. Water Sci. 11 (9) (2021).
[13] S.B. Alamne, et al., Mapping groundwater nitrate contaminant risk using the modified DRASTIC model: a case study in Ethiopia, Environ. Sys. Res. 11 (1) (2022).
[14] A.Z. Abiy, et al., Groundwater vulnerability analysis of the Tana sub-basin: an application of DRASTIC Index Method, in: Landscape Dynamics, Soils and Hydrological Processes in Varied Climates 435–461, 2016. Springer Geography.
[15] N. Kazakis, K.S. Voudouris, Groundwater vulnerability and pollution risk assessment of porous aquifers to nitrate: modifying the DRASTIC method using quantitative parameters, J. Hydrol. 525 (2015) 13–25.

[16] G.B. Zenebe, et al., Spatial analysis of groundwater vulnerability to contamination and human activity impact using a modified DRASTIC model in Elalla-Aynalem Catchment, Northern Ethiopia, Sustain. Water Res. Manag. 6 (3) (2020).
[17] A. Sepehrara, et al., Prediction of vulnerability map regarding to the dynamic parameters and land use changes, Environ. Earth Sci. 82 (21) (2023).
[18] D. Conway, The climate and hydrology of the upper Blue Nile River, Geogr. J. 166 (1) (2000) 49–62.
[19] A.A. Adem, et al., Hydrogeology of volcanic Highlands affects prioritization of land management practices, Water 12 (10) (2020).
[20] E. Abbate, et al., A one-million-year-old Homo cranium from the Danakil (Afar) Depression of Eritrea, Nature 393 (6684) (1998) 458–460.
[21] D. Ayalew, et al., Source, genesis, and timing of giant ignimbrite deposits associated with Ethiopian continental flood basalts, Geochem. Cosmochim. Acta 66 (8) (2002) 1429–1448.
[22] R. Pik, et al., The northwestern Ethiopian Plateau flood basalts: classification and spatial distribution of magma types, J. Volcanol. Geoth. Res. 81 (1–2) (1998) 91–111.
[23] A.S. Belay, et al., Investigation of interbasin groundwater flow using multiple approaches: the case of the Tana and Beles basins, Ethiopia, Hydrogeol. J. 31 (8) (2023) 2251–2270.
[24] J. Chorowicz, et al., The Tana basin, Ethiopia: intra-plateau uplift, rifting and subsidence, Tectonophysics 295 (3–4) (1998) 351–367.
[25] A.A. Moghaddam, S. Nouri Sangarab, A. Kadkhodaie Ilkhchi, Assessing groundwater vulnerability potential using modified DRASTIC in Ajabshir Plain, NW of Iran, Environ. Monit. Assess. 195 (4) (2023) 497.
[26] L. Aller, et al., DRASTIC: a standardized system for evaluating ground water pollution potential using hydrogeologic settings, in: U.S. Environment Protection Agency/600/2-87/035, 1987. Washington, DC, USA.
[27] A. Kumar, A.P. Krishna, Groundwater vulnerability and contamination risk assessment using GIS-based modified DRASTIC-LU model in hard rock aquifer system in India, Geocarto Int. 35 (11) (2018) 1149–1178.
[28] A. Wei, et al., Modified DRASTIC model for groundwater vulnerability to nitrate contamination in the Dagujia river basin, China, Water Supply 21 (4) (2021) 1793–1805.
[29] M. Hosseini, A. Saremi, Assessment and estimating groundwater vulnerability to pollution using a modified DRASTIC and GODS models (case study: Malayer plain of Iran), Civil Eng. J. 4 (2) (2018).
[30] S.S. Singha, et al., A GIS-based modified DRASTIC approach for geospatial modeling of groundwater vulnerability and pollution risk mapping in Korba district, Central India, Environ. Earth Sci. 78 (21) (2019).
[31] M. Torkashvand, et al., Groundwater vulnerability to nitrate contamination from fertilizers using modified DRASTIC frameworks, Water 15 (17) (2023).
[32] T. De Vargas, R. Belladona, M.E.R. de Souza, Serra Geral fractured aquifer and the uncertainties of geospatial models: a case study in the caxias fault zone, J. S. Am. Earth Sci. 124 (2023).
[33] T. De Vargas, R. Belladona, M.E.R.d. Souza, Hydrogeology of fractured aquifers: application of consistency indexes for the validation of geospatial mathematical models, Geocîencias - Unesp 41 (2022) 391–404.
[34] A. Al-Rawabdeh, et al., Modeling the risk of groundwater contamination using modified DRASTIC and GIS in Amman-Zerqa Basin, Jordan, Open Eng. 4 (3) (2014).
[35] R. Thapa, et al., Sensitivity analysis and mapping the potential groundwater vulnerability zones in Birbhum district, India: a comparative approach between vulnerability models, Water Sci. 32 (1) (2018) 44–66.
[36] G. Piscopo, Groundwater Vulnerability Map, Explanatory Notes, Castlereaght Catchment. NSW, Department of Land and Water Conservation, Australia, 2001.
[37] H.R. Jr, A.P. Viero, Groundwater vulnerability assessment in coastal plain of Rio Grande do Sul State, Brazil, using drastic and adsorption capacity of soils, Environ. Geol. 52 (5) (2007) 819–829.
[38] L. Balaji, et al., Groundwater vulnerability mapping using the modified DRASTIC model: the metaheuristic algorithm approach, Environ. Monit. Assess. 193 (1) (2021) 25.
[39] M.H.R. Moghaddam, et al., Groundwater vulnerability assessment using the DRASTIC model under GIS platform in the Ajabshir Plain, southeast coast of Urmia Lake, Iran, Arabian J. Geosci. 11 (19) (2018).
[40] T. Gashaw, et al., Evaluating the effectiveness of best management practices on soil erosion reduction using the SWAT model: for the case of Gumara watershed, Abbay (upper Blue nile) basin, Environ. Manag. 68 (2) (2021) 240–261.
[41] W. Abuhay, T. Gashaw, L. Tsegaye, Assessing impacts of land use/land cover changes on the hydrology of Upper Gilgel Abbay watershed using the SWAT model, J. Agri. Food Res. 12 (2023).
[42] B.F. Admas, et al., Identification of soil erosion hot-spot areas for prioritization of conservation measures using the SWAT model in Ribb watershed, Ethiopia, Res. Environ. Sustain. 8 (2022).
[43] M.S. Siddik, et al., The impact of land use and land cover change on groundwater recharge in northwestern Bangladesh, J. Environ. Manag. 315 (2022) 115130.
[44] I. Ahmed, Y. Nazzal, F. Zaidi, Groundwater pollution risk mapping using modified DRASTIC model in parts of Hail region of Saudi Arabia, Environ. Eng. Res. 23 (1) (2018) 84–91.
[45] B.D. Lindsey, et al., Thirty years of regional groundwater-quality trend studies in the United States: major findings and lessons learned, J. Hydrol. 627 (2023).
[46] D. Machiwal, P.K. Singh, K.K. Yadav, Estimating aquifer properties and distributed groundwater recharge in a hard-rock catchment of Udaipur, India, Appl. Water Sci. 7 (6) (2017) 3157–3172.
[47] T. Gashaw, et al., Evaluation and prediction of land use/land cover changes in the Andassa watershed, Blue Nile Basin, Ethiopia, Environ. Sys. Res. 6 (1) (2017).
[48] A.G. Mengistu, et al., Modeling impacts of projected land use and climate changes on the water balance in the Baro basin, Ethiopia, Heliyon 9 (3) (2023) e13965.
[49] T.W. Yitbarek, J.R.U. Wilson, K. Dehnen-Schmutz, Investigating tree planting in Ethiopia and the extent to which scheme implementation aligns with good governance practices, J. Environ. Manag. 373 (2024) 123475.
[50] T. Gashaw, et al., Evaluating potential impacts of land management practices on soil erosion in the Gilgel Abay watershed, upper Blue Nile basin, Heliyon 6 (8) (2020) e04777.
[51] H. Huan, J. Wang, Y. Teng, Assessment and validation of groundwater vulnerability to nitrate based on a modified DRASTIC model: a case study in Jilin City of northeast China, Sci. Total Environ. 440 (2012) 14–23.
[52] R. Lathamani, et al., Evaluation of aquifer vulnerability using drastic model and GIS: a case study of Mysore city, Karnataka, India, Aquatic Procedia 4 (2015) 1031–1038.
[53] A.M. Al-Abadi, A.M. Al-Shamma'a, M.H. Aljabbari, A GIS-based DRASTIC model for assessing intrinsic groundwater vulnerability in northeastern Missan governorate, southern Iraq, Appl. Water Sci. 7 (1) (2014) 89–101.
[54] D.C. Jhariya, et al., Assessment of groundwater vulnerability to pollution by modified DRASTIC model and analytic hierarchy process, Environ. Earth Sci. 78 (20) (2019).
[55] R. Khan, D.C. Jhariya, Assessment of groundwater pollution vulnerability using GIS based modified DRASTIC model in Raipur city, Chhattisgarh, J. Geol. Soc. India 93 (3) (2019) 293–304.